High resolution Magnetization Transfer Ratio (MTR) mapping in Multiple Sclerosis

Ali Al-Radaideh[1], Olivier Mougin[1], Su-Yin Lim[2], Christopher Tench[2], Cris Constantinescu[2], Penny Gowland[1].
1-Sir Peter Mansfield MR centre, University of Nottingham 2-Clinical Neurology, University of Nottingham

Introduction: Multiple Sclerosis (MS) is a condition that affects young adults typically aged 20-40 years, and involves inflammation and demyelination of neural axons in the brain and nervous system. Magnetization transfer (MT) imaging studies the interaction between water and macromolecular (e.g.Protein in Myelin) protons and can be a useful in studying the changes in normal appearing white matter (NAWM) and grey matter (GM). It has the ability to detect the activity of disease and monitor its progression [1]. The destruction of myelin of neural fibers in MS disease results in a reduction in magnetization transfer process between water and myelin which correlates well with physical disability in MS patients [2]. MT imaging at 7T benefits from high spatial resolution due to increased signal to noise ratio. Limitations due to high Specific Absorption Rate (SAR) can be resolved using an MT prepared turbo field echo sequence (MT-TFE) with pulsed saturation pulse. Previous work [3] has shown that the MTR distribution of normal appearing white matter (NAWM) in the brains of MS patients is different from that of healthy control subjects and varies with distance from lesion site. Here, we measure the distribution of MTR values at 7T, comparing WM in healthy controls with normal appearing WM in MS patients.
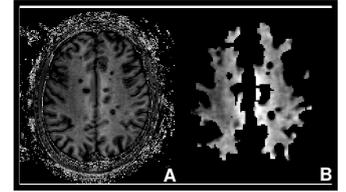

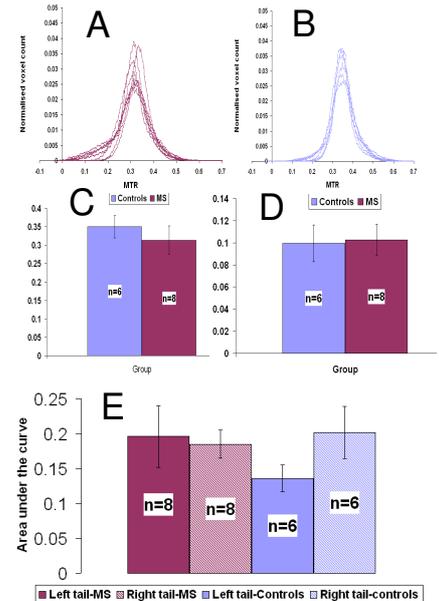Fig.1: (A) MTR map (B) MTR map of segmented NAWM

Fig.2: (A) MTR distribution in MS subjects (B) MTR distribution in Healthy subjects. (C)-(E) statistical analysis of MTR values in both MS and healthy subjects

Methods: Eight MS patients with Clinically Isolated Syndrome (CIS) (early MS) were recruited from Nottingham University Hospital. Six age and sex matched healthy volunteers were also recruited, and both groups were consented according to local ethics approval. Scanning was performed on a 7T Philips Achieva system. The scan protocol at 7T included 3D MPRAGE, 2D multi-slice FLAIR, T2*-w. T1 maps were derived using data acquired using a range of MPRAGE images (200x170x73 mm^3 FOV, 1.25 mm isotropic voxels, TE=3.2 ms; TR=6.9 ms; TFE shots=16;58 slices; SENSE factor = 2, scan time per TI =2 min) at 7 different inversion times (150, 300, 500, 800, 1200, 1800, 2500 ms). 3DMT-TFE sequence (1x1x1.5mm resolution; 220 x 220 x 30 mm^3 FOV; TE=5.7 ms; TR=9.8 ms; TFE factor 256; 20 slices; total scan time =8:22min). MT images were acquired in three dynamics giving signals for no saturation pulse (S_{0-}) and for two different frequency offsets relative to water frequency (S_{MT+} for offset of +1100Hz and S_{MT-} for offset of -1100 Hz). Both positive and negative frequency offsets were co-registered to S_0 image and the MTR maps were then calculated on voxel by voxel basis as shown in the box. where MTR$_+$/ MTR$_-$ is the magnetisation transfer ratio when a saturation RF pulse is applied at positive/negative offset to water frequency (S_{MT+}). The MPRAGE image from the T1 measurement set, near the null point was used in SPM5 [4] to segment the grey and white matter. The segmented

$$MTR_+ = (S_{MT0} - S_{MT+})/S_{MT0}$$
$$MTR_- = (S_{MT0} - S_{MT-})/S_{MT0}$$
$$MTR_{mean} = [MTR_+ + MTR_-]/2$$

white matter was displayed as a probability map which was then converted to a mask. This mask was used to define areas of healthy appearing white matter in all three MTR maps using ImageJ [5]. We ensured that these WM areas excluded any detectable WM MS lesions. The histogram of MTR$_{mean}$ values in the healthy appearing WM was normalised to the number of pixels in the mask and plotted. The mean, median, mode, Full Width at Half Maximum (FWHM), peak height, and area under the curve of left and right tails of histograms were calculated. The interval of MTR values that covers the left tail was selected to be from 0.001to the first MTR value that corresponds to the half maximum. The interval of MTR values that covers the right tail, on the other hand, was selected to be from the second MTR value that corresponds to the half maximum to 1.0.

Results: Fig (1-A) shows some hypointense MS lesions. A segmented white matter of the same MTR map with lesions being excluded is shown in fig (1-B). Fig. 2 (A and B) show a distribution of MTR value in normal appearing WM (after lesions were excluded) of MS and healthy subjects respectively. The mean of the MTR values of NAWM in brains of MS patients is significantly (p<0.05) different from that in healthy brains as shown in fig 2-C. The FWHM (average ± std across subjects) of MTR values is shown in fig 2-D. The area under the curve of left and right tails are shown in fig 2-E. The Average of median, FWHM, mode, peak height of MTR values in MS and healthy controls showed a similar trend with no significant difference.

Discussion: Although the data showed that accurate MTR maps can be acquired with high spatial resolution. Our masking procedure eliminated grey matter, CSF and lesions so that MTR histograms comprising the healthy appearing white matter could be formed. Our results agree with previous studies at lower field strength and suggest that there is a difference in the MTR distribution between healthy appearing WM in MS patients and normal volunteers, but it is worth noting that subjects only had CIS (early MS). Future work will consider the difference between the MTR$_+$ and MTR$_-$ signals and focus on calculating any correlation between MTR values with other MRI parameters that can be measured from the used protocol such as T1, T2*, cortical thickness as well as with clinical status of MS subjects (e.g physical disability). Further analysis including showing the spatial distribution of MTR values within the NAWM and relative to MS lesions locations. The latter could investigate the distribution of MTR values relative to MS lesion using concentric rings.

References: 1) Marco Rovaris et al, *British Medical Bulletin*. 2003 **65**: p.133–144.. 2)Mohit Neema, et al. Neurotherapeutics 2007. **4**: p. 602–617. 3) H. Vrenken, et al., AJNR, 2006. **27**: p. 2005-2011 4) http://www.fil.ion.ucl.ac.uk/spm/software/spm5/) .5) (http://rsb.info.nih.gov/ij/).